BIOCHEMISTRY
including biophysical chemistry & molecular biology

Article

pubs.acs.org/biochemistry

Allocrite Sensing and Binding by the Breast Cancer Resistance Protein (ABCG2) and P-Glycoprotein (ABCB1)

Yanyan Xu,[†,‡] Estefanía Egido,[†,§,∥] Xiaochun Li-Blatter,[†] Rita Müller,[†] Gracia Merino,[§,∥] Simon Bernèche,[†,‡] and Anna Seelig*[,†]

[†]University of Basel, Biozentrum, Klingelbergstrasse 50/70, CH-4056 Basel, Switzerland

[‡]SIB Swiss Institute of Bioinformatics, Klingelbergstrasse 61, CH-4056 Basel, Switzerland

[§]INDEGSAL, Campus Vegazana s/n, University of Leon, 24071 Leon, Spain

[∥]Department of Biomedical Sciences-Physiology, Veterinary Faculty, Campus Vegazana s/n, University of Leon, 24071 Leon, Spain

Supporting Information

ABSTRACT: The ATP binding cassette (ABC) transporters ABCG2 and ABCB1 perform ATP hydrolysis-dependent efflux of structurally highly diverse compounds, collectively called allocrites. Whereas much is known about allocrite−ABCB1 interactions, the chemical nature and strength of ABCG2−allocrite interactions have not yet been assessed. We quantified and characterized interactions of allocrite with ABCG2 and ABCB1 using a set of 39 diverse compounds. We also investigated potential allocrite binding sites based on available transporter structures and structural models. We demonstrate that ABCG2 binds its allocrites from the lipid membrane, despite their hydrophilicity. Hence, binding of allocrite to both transporters is a two-step process, starting with a lipid−water partitioning step, driven mainly by hydrophobic interactions, followed by a transporter binding step in the lipid membrane. We show that binding of allocrite to both transporters increases with the number of hydrogen bond acceptors in allocrites. Scrutinizing the transporter translocation pathways revealed ample hydrogen bond donors for allocrite binding. Importantly, the hydrogen bond donor strength is, on average, higher in ABCG2 than in ABCB1, which explains the higher measured affinity of allocrite for ABCG2. $\pi-\pi$ stacking and π−cation interactions play additional roles in binding of allocrite to ABCG2 and ABCB1. With this analysis, we demonstrate that these membrane-mediated weak electrostatic interactions between transporters and allocrites allow for transporter promiscuity toward allocrites. The different sensitivities of the transporters to allocrites' charge and amphiphilicity provide transporter specificity. In addition, we show that the different hydrogen bond donor strengths in the two transporters allow for affinity tuning.

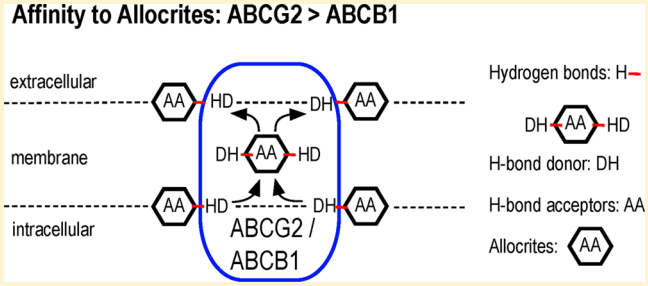

The human breast cancer resistance protein (ABCG2, BCRP)[1] and P-glycoprotein (ABCB1, Pgp, MDR1)[2] are integral membrane proteins that belong to the family of ATP binding cassette (ABC) transporters, present in prokaryotes and eukaryotes. Like ABCB1,[3] ABCG2[4] performs ATP hydrolysis-dependent efflux of a large number of structurally and functionally unrelated compounds,[5−7] collectively called allocrites.[8] The two transporters are constitutively produced in most cells. In particular, high levels are found in protective membrane barriers, as well as in cancer cells, where the transporters strongly contribute to multidrug resistance (MDR).[3,4,9] The transporters thus fulfill important functions in cellular detoxification. In addition, ABCG2 serves rather specific, physiological functions, e.g., in blood group determination, and stem cell development.[10]

Whereas ABCB1 (∼170 kDa) functions as a monomer, consisting of two cytosolic nucleotide binding domains (NBDs) and two transmembrane domains (TMDs), ABCG2 (∼75 kDa) is a half-transporter that consists of only one NBD and one TMD and functions as a homodimer.[4,11] It was also proposed that ABCG2 could function as a homotetramer.[12,13] Crystal structures of two eukaryotic homologues of human ABCB1, murine ABCB1 (Abcb1a, Mdr3)[14,15] and CmABCB1 from *Cyanidioschyzon merolae*,[16] both in the apo form, revealed a wide-open inward-facing state. The apo form of ABCG2 in two-dimensional crystals also adopted an inward-facing structure, as shown by cryoelectron microscopy.[17] Despite functional and structural similarities, ABCB1 and ABCG2 exhibit only little protein sequence identity in the NBDs (∼20%) and practically no sequence identity in the TMDs.[11] Nevertheless, the two proteins share certain allocrites.[18−20] It is therefore of great interest to analyze the molecular basis of allocrite recognition by ABCB1 and ABCG2.

Binding of allocrite to ABCB1 has been intensively investigated. A first fundamental finding was that allocrites

Received: June 12, 2015
Revised: September 18, 2015
Published: September 18, 2015

DOI: 10.1021/acs.biochem.5b00649
Biochemistry 2015, 54, 6195−6206

partition into the lipid membrane before binding to ABCB1,[21] which is due to their hydrophobicity and amphiphilicity.[22,23] Therefore, binding of allocrite to ABCB1 is best described as a two-step process,[24,25] comprising a membrane partitioning step driven mainly by hydrophobic interactions and a transporter binding step occurring from within the lipid environment. The analysis of a large number of allocrite structures combined with functional data revealed that the binding step must be driven by weak electrostatic interactions, including hydrogen bond formation,[26,27] $\pi-\pi$ stacking, and cation$-\pi$ interactions,[28] generally decreasing in the order given. The concept of binding of allocrite to ABCB1 via hydrogen bond formation between hydrogen bond acceptors (HBAs) in allocrites and hydrogen bond donors (HBDs) in TMDs was verified with diverse drugs[24,29] and, in a more systematic manner, with detergents carrying variable numbers of HBAs in their polar parts.[23,30,31] In this context, it is interesting to note that allocrites binding to ABCB1 also bind to water-soluble MDR gene regulators, however, with a different binding mechanism. The aqueous phase favors hydrophobic and $\pi-\pi$ stacking allocrite$-$protein interactions,[32] whereas hydrogen bonding plays a minor role.

A second important finding was that the binding sites of ABCB1, located within the TMDs in the cytoplasmic leaflet of the membrane, can simultaneously harbor more than one allocrite.[33−39] Crystallographic snapshots of the cyclic peptide, QZ59-RRR, and particularly its stereoisomer, QZ59-SSS, bound to ABCB1,[14] support the findings described above. ATPase activity of ABCB1 measured as a function of allocrite concentration in inside-out plasma membrane vesicles[33] and live cells[24,40] yielded bell-shaped activity curves that can be well fitted with a two-site binding model that assumes activation at low allocrite loads and inhibition at high allocrite loads in the transporter.[33] The inhibitory part of the activity curve at high allocrite concentrations could be unambiguously attributed to transporter deceleration (i.e., transporter inhibition)[20] using an ADP-to-ATP regeneration assay.[41]

So far, much less about the interaction of allocrites with ABCG2 is known. Inhibitors of ABCG2 were shown to carry HBAs for an interaction with the transporter and to be amphiphilic and hydrophobic.[42] Conversely, activators of ABCG2 were shown to be hydrophilic, nonamphiphilic, and often highly charged,[20] suggesting a weak tendency to partition into the lipid membrane. Provided the membrane solubility of allocrites was sufficiently high, the ABCG2$-$ATPase activity measured as a function of allocrite concentration yielded bell-shaped activity curves, suggesting the same type of activation/inhibition mechanism as for ABCB1.[20]

A number of principle questions regarding ABCG2$-$allocrite interactions are still unanswered. (i) Is binding of allocrite to ABCG2 mediated by the aqueous phase, or is it mediated by the lipid phase? The answer to this question is most relevant because, as shown above by the comparison of transporters and gene regulators,[32] the environment determines the nature of allocrite$-$protein interactions. (ii) Which are the physical forces underlying binding of allocrite to ABCG2? (iii) What is the physical reason for the higher affinity of allocrites for ABCG2 than for ABCB1?[20]

To answer these questions, we combined a functional analysis of binding of allocrite to the two transporters, using a probe set of 39 diverse compounds, with a structural analysis of the potential binding regions in the TMDs of the two transporters. As a basis for the functional analysis, we used ABCB1 and ABCG2 ATPase activity measurements performed as a function of allocrite concentration from a previous study[20] (30 allocrites) and completed the set with nine further compounds. The free energy of allocrite binding from water to the transporter, ΔG^0_{tw}, was derived from concentrations of half-maximal transporter activation, K_1. The free energy of allocrite binding from the lipid membrane to the transporter, ΔG^0_{tl} (i.e., effective allocrite binding affinity), was assessed as the difference between the former and the free energy of lipid$-$water partitioning, ΔG^0_{lw}, derived from surface activity measurements. For the structural analysis, we used the murine Abcb1 (Abcb1a) structure, open to the cytosol,[15] and a model of ABCB1 based on the structure of Sav1866[43] with two molecules of ADP bound, open to the extracellular space. Given the low degree of sequence homology between ABCG2 and transporters of known structure,[10,17] only the primary and secondary structures were considered.

With this analysis, we demonstrate that despite the hydrophilicity of typical ABCG2 activators, allocrite sensing and binding by ABCG2 are membrane-mediated. ABCG2 binds its allocrites mainly via the formation of hydrogen bonds between hydrogen bond-donating amino acid residues (HBDs) in the TMDs and HBAs in allocrites. The significantly higher affinity of allocrites for ABCG2 than for ABCB1 can be explained by the higher hydrogen bond donor strength of HBDs. Charged residues are shown to be important for sensing and gating and to lesser extent to binding. This first quantitative analysis of allocrite sensing and binding by ABCG2 in comparison to that by ABCB1 yields insights into the apparent paradox of ABC transporter promiscuity and specificity.

MATERIALS AND METHODS

Compounds. Cimetidine, ciprofloxacin, hydrocortisone (cortisol), 8-(4-chlorophenylthio)adenosine 3′,5′-cyclic monophosphate sodium salt (CPT-cAMP), daunorubicin·HCl, dexamethasone, digoxin, enrofloxacin, β-estradiol, etoposide, famotidine, forskolin, glibenclamide, Ko143, methotrexate, mitoxantrone·2HCl, moxifloxacin·HCl, nizatidine, norfloxacin, pefloxacin mesylate, prazosin·HCl, progesterone, promazine·HCl, ranitidine·HCl, (−)-riboflavin, sulfasalazine, tamoxifen, testosterone, (*R*/*S*)-verapamil·HCl, colchicine, L-ascorbic acid (ascorbic acid), maltose, and sodium hexanoate were purchased from Sigma-Aldrich (Steinheim, Germany). Cyclosporin A was a gift from Novartis (Basel, Switzerland). Complete EDTA-free protease inhibitor cocktail tablets were obtained from Roche Diagnostics (Mannheim, Germany), and 1,4-dithio-DL-threitol (DTT) and Tris ultrapure were from AppliChem (Darmstadt, Germany). Bicinchoninic acid (BCA) protein assay reagents were from Pierce (Rockford, IL). All other chemicals were from Sigma-Aldrich or Merck. PBS, DPBS, cell culture media, including Dulbecco's modified Eagle's medium (DMEM) with and without pyruvate, and other compounds required for cell culture such as fetal bovine serum (FBS), 0.05% trypsin with EDTA, L-glutamine, and antibiotics were purchased from Gibco, Invitrogen (Basel, Switzerland). Cyclohexyl-methyl-β-D-maltopyranoside (Cymal-1), 6-tetradecyl-β-D-maltopyranoside (C_6-malt), and *n*-octylphosphocholine (Fos-choline-8) were obtained from Anatrace (Maumee, OH), and 1,2-dicaproyl-*sn*-glycero-3-phosphocholine (DHPC) was from Avanti Polar Lipids (Alabaster, AL).

Cell Lines and Cell Culture. Mouse embryo fibroblasts stably transfected with the human MDR1 gene (NIH-MDR1-G185) were a generous gift from M. M. Gottesman and S. V. Ambudkar (National Institutes of Health, Bethesda, MD). Cells were grown as described previously.[44,45]

DOI: 10.1021/acs.biochem.5b00649
Biochemistry 2015, 54, 6195−6206

Plasma Membrane Vesicles. Inside-out vesicles of NIH-MDR1-G185 cell membranes were prepared as described previously.[40] Depending on the preparation, the protein content of the plasma membrane vesicles was determined to be 6−11.1 mg/mL by means of a BCA assay, using bovine serum albumin as a standard. The number of ABCB1 molecules per cell was previously determined to be approximately 1.95×10^6,[46] which amounts to approximately 1.1% of the total protein content.[40] Vesicles exhibited a predominantly inside-out orientation. Inside-out plasma membrane vesicle preparations from isolated mammalian cells containing human ABCG2 (ABCG2-M-ATPase) with a protein content of 5 mg/mL (BCA assay) were obtained from SOLVO Biotechnology (Budapest, Hungary). The number of ABCG2 molecules per cell was determined to be $\geq 3.5 \times 10^6$,[47] which amounts to an ABCG2 protein content somewhat higher than that obtained for ABCB1 in NIH-MDR1-G185 cells.

Analysis of Kinetic Data. The rate of ATP hydrolysis, V_A (or ATPase activity), as a function of allocrite concentration, C_A, in solution yielded bell-shaped curves that were analyzed with a two-site binding model (eq 1) that assumes activation upon occupation of a first binding site (or region) and inhibition upon occupation of a second binding site (or region)[33]

$$V_A = \frac{K_1K_2V_0 + K_2V_1C_A + V_2{C_A}^2}{K_1K_2 + K_2C_A + {C_A}^2} \quad (1)$$

where V_0 is the basal activity in the absence of allocrites, V_1 is the maximal transporter activity (if only activation occurred), V_2 is the minimal activity at a high allocrite concentration, K_1 is the half-maximal activation, and K_2 is the half-maximal inhibition. The equation is based on the concept of uncompetitive inhibition (assuming that the same compound can act as an allocrite and inhibitor depending on the concentration applied) (for details, see ref 24). As discussed below, this model can also be applied to ABCG2 ATPase activity measurements.

Membrane-Mediated Allocrite Binding. Binding of allocrite to ABCB1 was shown to be membrane-mediated.[24,25] The binding constant of an allocrite from water to the first binding site of ABCB1 (P), $K_{tw1,P}$, can therefore be described as the product of the lipid−water partition coefficient, K_{lw}, and the allocrite binding constant from the lipid phase to the transporter, $K_{lt1,P}$

$$K_{tw1,P} = K_{lw}K_{tl1,P} \quad (2)$$

The allocrite binding constant from water to the first binding site of the transporter, K_{tw} (or more generally K_x), and the corresponding free energy of binding, ΔG^0_{tw1} (or more generally, ΔG^0_x), are correlated as follows

$$\Delta G^0_x = -RT \times \ln(K_xC_w) \quad (3)$$

where C_w is the concentration of water (C_w = 55.3 mol L^{-1} at 37 °C). The free energy of allocrite binding from water to the first binding site of the transporter ABCB1, $\Delta G^0_{tw1,P}$, can then be defined as the sum of the free energy of allocrite lipid−water partitioning, ΔG^0_{lw}, and the free energy of allocrite binding from the lipid membrane to the first binding site of ABCB1, $\Delta G^0_{tl1,P}$ (eq 3)

$$\Delta G^0_{tw1,P} = \Delta G^0_{lw} + \Delta G^0_{tl1,P} \quad (4)$$

An analogous equation can be formulated for the second binding site.

Lipid−Water Partition Coefficient. The apparent free energy of lipid−water partitioning, ΔG^0_{lw}, was determined by measuring the free energy of air−water partitioning, ΔG^0_{aw}, and cross-sectional area A_D of the molecule[48,49]

$$\Delta G^0_{lw} = \Delta G^0_{aw} + \pi_M N_A A_D \quad (5)$$

where π_M is the lateral membrane packing density and N_A Avogadro's number. The measured cross-sectional areas, A_D meas, were used if possible. Exceptions were made for amphiphilic hydrophobic compounds **5** (progesterone) and **12** (testosterone), which aggregated at higher concentrations in solution, and nonamphiphilic compounds **26** (ciprofloxacin), which also aggregated at higher concentrations, and **20** (sulfasalazine), which was too large, because of charge repulsion effects. In the case of amphiphilic molecules, the calculated minimum areas, A_D min/c, and in the case of nonamphiphilic compounds the calculated maximum areas, A_D max/c, were taken for calculation of lipid−water partition coefficients (for data, see Table S1 and ref 20).

It has to be noted that the apparent lipid−water partition coefficient, K_{lw}, changes with concentration for charged compounds.[50] The advantage of using surface activity measurements for assessment of lipid−water partition coefficients is twofold. First, the air−water partition coefficient approximately corresponds to the inverse of the concentration of half-maximal activation ($K_{aw} \approx 1/K_1$). Using the air−water partition coefficient, K_{aw}, therefore yields the apparent lipid−water partition coefficient, K_{lw}, at the transporter-relevant concentration, K_1. Moreover, knowledge of the air−water partition coefficient, K_{aw}, allows assessment of the lipid−water partition coefficient, K_{lw}, at any lateral membrane packing density, π_M.

Modeling. Swiss model (http://swissmodel.expasy.org) was used for homology modeling of ABCB1 in an outward-facing conformation based on the structure of Sav1866 with nucleotides bound.[43] In the apo-ABCB1 (Abcb1a) structure,[14] which is open to the cytosol, the linker between the two pseudosymmetric half-molecules is missing, and hence, there are two chains as in Sav1866. Therefore, the two half-molecules of ABCB1 were modeled separately on the basis of the structures of the two subunits of Sav1866. Images were made with VMD software support. VMD is developed with NIH support by the Theoretical and Computational Biophysics group at the Beckman Institute, University of Illinois at Urbana-Champaign (http://www.ks.uiuc.edu/Research/vmd/).

Sequence Comparison for ABCB1 and ABCG2. We analyzed the number and nature of residues with HBD groups, including cysteine (Cys), tyrosine (Tyr), tryptophan (Trp), asparagine (Asn), glutamine (Gln), serine (Ser), and threonine (Thr), and the number of phenyl residues (Phe) in the TMDs of ABCB1 and ABCG2. For this purpose, we determined the median plane of the bilayer surrounding ABCB1 in its apo conformation open to the cytosol using Protein Data Bank (PDB) entry 4m1m of the OPM (Orientation of Proteins in Membranes) database (http://opm.phar.umich.edu). Considering the length of a palmitoyloleoylphosphatidylcholine (POPC) molecule of approximately 25 Å, the boundaries of the membrane were set to be 25 Å above and below the median plane of the bilayer. The membrane-embedded section of the protein (TMD) was then used for analysis. According to the sequence alignment in a previous investigation,[17] the corresponding sequence segments of ABCG2 were obtained and assumed also to correspond to the TMD.

DOI: 10.1021/acs.biochem.5b00649
Biochemistry 2015, 54, 6195−6206

Table 1. Kinetic Parameters Derived from ATPase Activity Measurements as a Function of the Concentration of Potential ABCB1 and ABCG2 Allocrites[a]

		ABCB1				ABCG2			
	compound	K_1 (μM)	K_2 (μM)	V_1 (%)	V_2 (%)	K_1 (μM)	K_2 (μM)	V_1 (%)	V_2 (%)
31	maltose	ni	ni	ni	ni	ni	ni	100	100
32	ascorbic acid	ni	ni	ni	ni	ni	ni	100	100
33	heptanoic acid	ni	ni	ni	ni	ni	ni	100	100
34	C12EO8	0.904	14.9	191	0.60	nd	6.93	~100	0
35	CHAPS	nd	85.6	98	78	nd	24.06	~100	42
36	C6-malt	nd	3.30×10^4	100	0	nd	4.6×10^3	~100	43
37	Cymal-1	nd	8.61×10^4	100	95	nd	1.51×10^4	~100	0
38	DHPC	3.20×10^3	nd	243	nd	nd	727.87	~100	19
39	fos-choline-8	122.9	1.53×10^4	127	0	nd	2.67×10^3	~100	49

[a]Abbreviations: ni, no interaction; nd, not determined.

Table 2. Thermodynamic Parameters of Potential ABCB1 and ABCG2 Allocrites Obtained by Measuring the Gibbs Adsorption Isotherm[a]

	compound	MW (g/mol)	A_D (Å^2)	K_{aw} (mM^{-1})	CMC_D (mM)	HBA (EU)	amphiphilicity	charge at pH 7.0
31	maltose	342.30	nsa	nsa	nsa	3	n-am	0
32	ascorbic acid	176.12	nsa	nsa	nsa	2	n-am	−
33	heptanoic acid	130.19	nsa	nsa	nsa	1	am	−
34	C12EO8	538.8	71.9	7300	0.0953	8	am	0
35	CHAPS	614.9	83.6	78.8	4.85	2.5	am	−/+
36	C6-malt	426.4	65.7	0.684	210	4	am	0
38	DHPC	481.6	92.6	432	1.9	7.5	am	−/+
39	fos-choline-8	295.4	41.4	3.32	114	3.5	am	−/+

[a]Abbreviations: n-am, nonamphiphilic compounds; am, amphiphilic compounds; nsa, no surface activity.

Moreover, we investigated the number and nature of charged residues at the membrane−cytosol interface, including the cationic arginine (Arg), lysine (Lys), and histidine (His), and the anionic glutamic acid (Glu), and aspartic acid (Asp). The interface considered is 10 Å above the membrane−cytosol boundary, i.e., between 15 and 25 Å below the median plane of the bilayer. The corresponding sequence segments of ABCG2 were again obtained from the previous sequence alignment[17] assuming that they are also at the interface.

Glossary. According to the definition of Holland and Blight,[8] an allocrite (or transport substrate) is a compound that appears as transported in a transport assay. The transport assay (see, e.g., ref 51) reveals the net flux (or apparent transport) that is the sum of effective, active transport, and passive diffusion of compounds across the membrane.[52] Whereas effective, active transport is proportional to ABC-ATPase activity, apparent transport (measured in transport assays) is not. For mechanistic analyses of transporter activity, effective (not apparent) transport has to be considered. In the following, the term allocrite therefore refers to effective allocrites, which can be determined by ATPase activity measurements (see also refs 23 and 31).

Most inhibitors of ABCB1 and ABCG2 are allocrites that are able to reduce the rate of ATP hydrolysis and concomitantly the rate of effective transport (for detailed information, see ref 20). Typical examples of ABCB1 inhibitors are cyclosporin A and verapamil. The former inhibits ABCB1 already at low concentrations, because of its high affinity for the transporter. The latter activates ABCB1 at low concentrations and inhibits it only at high concentrations, where the second binding site becomes occupied.[30]

RESULTS AND DISCUSSION

Allocrite Binding Is Membrane-Mediated for Both Transporters. The structure of ABCG2 in the apo state is wide open to the cytosol,[14,15,17] which suggests the possibility of allocrite access from the aqueous, cytosolic phase to the transporter. Because allocrites for ABCG2 are more hydrophilic than those for ABCB1, we tested whether access to ABCG2 is possible directly from the aqueous phase. For this purpose, we used water-soluble compounds for which membrane insertion could not be measured but which carry the relevant HBAs required for an interaction with the transporters (see Common Recognition Patterns for ABCB1 and ABCG2), on one hand, and analogous compounds modified by a membrane anchor, on the other. The compounds (**31**−**39**) are summarized in Table 1, together with the kinetic ATPase activity data, and in Table 2, together with the respective physicochemical constants. Titration of ABCG2 with increasing concentrations of the water-soluble compounds, including maltose among others, had no effect on ATPase activity. Conversely, the electrically neutral amphiphilic maltoside, C_6-malt, and other more hydrophobic amphiphiles showed significant membrane partitioning and inhibited ABCG2 well below their CMC, as expected in analogy to other amphiphilic compounds (Table 1, compounds **1**−**14**, in ref 20). Access to the transporter directly from the aqueous phase seems therefore highly unlikely for ABCG2. In conclusion, a hydrophobic moiety is required to drive the allocrite into the lipid bilayer, from where it can access the transporter binding site, located in the cytosolic leaflet of the membrane.

Allocrite binding thus occurs in two steps, a lipid−water partitioning step, followed by a transporter binding step, which takes place in the lipid phase. As shown previously for ABCB1 (see eq 4), the free energy of allocrite binding from water to ABCG2 (B), $\Delta G^0_{tw1,B}$, can thus be expressed as the sum of the free

DOI: 10.1021/acs.biochem.5b00649
Biochemistry 2015, 54, 6195−6206

energy of lipid−water partitioning of the allocrite ΔG^0_{lw} and the free energy of allocrite binding to ABCG2 from the lipid membrane $\Delta G^0_{tl1,B}$

$$\Delta G^0_{twl,B} = \Delta G^0_{lw} + \Delta G^0_{tl1,B} \quad (6)$$

An analogous equation can be formulated for the second binding site (not shown). As noted above, the free energy of lipid−water allocrite partitioning, ΔG^0_{lw}, is due mainly to hydrophobic interactions, whereas the free energy of transporter−lipid allocrite binding, $\Delta G^0_{tl1,B}$, is likely to be due to hydrogen bond formation and other weak electrostatic interactions. This hypothesis is tested in the following.

The Affinity for Transporters Increases with the Number of HBAs per Allocrite. We experimentally tested whether the free energy of binding, $\Delta G^0_{tl1,B}$, which reflects the direct interaction of the allocrite with the transporter, indeed correlates with the number of HBAs per allocrite. For this purpose, we plotted the free energy of binding of an allocrite from water to the first binding site of the transporter (or transporter−water binding), for ABCB1 and ABCG2, $\Delta G^0_{tw1,P}$ and $\Delta G^0_{tw1,B}$, respectively, versus the free energy of air−water partitioning, ΔG^0_{aw}, of the allocrites. As seen in panels A and B of Figure 1, an approximately linear correlation between the two parameters with a slope of 1 is observed for ABCB1 allocrites as well as for ABCG2 allocrites

$$\Delta G^0_{tw1} \approx \Delta G^0_{aw} \quad (7)$$

Although the correlation given in eq 7 has a phenomenological rather than a rigorous physicochemical background, it helps in understanding allocrite−transporter interactions in more detail.

Rewriting eq 7, by taking into account eq 5, yields

$$\Delta G^0_{tw1} \approx \Delta G^0_{aw} = \Delta G^0_{lw} - \pi_M N_A A_D \quad (8)$$

According to eq 8, the free energy of allocrite binding from water to the transporter, ΔG^0_{tw1}, depends on two terms, the free energy of lipid−water partitioning, ΔG^0_{lw}, and a term comprising the cross-sectional area of the molecule, A_D, whereby the lateral membrane packing density, π_M, is assumed to remain approximately constant. Combining eq 4 (or eq 6) with eq 8 yields

$$\Delta G^0_{tl1} \approx -\pi_M N_A A_D \quad (9)$$

Hence, the free energy of allocrite binding from the lipid membrane to the first binding site of the transporter, ΔG^0_{tl1}, is predicted to be proportional to the cross-sectional area of the allocrites, A_D, for ABCG2 as well as for ABCB1.[23,24,30,31] As seen in panels A and B of Figure S1, a broad linear correlation between the free energy of binding, ΔG^0_{tl1}, and the cross-sectional area, A_D, is indeed observed for allocrites of both transporters. As shown in Figure S1C (see also ref 53), the number of HBAs generally increases with increasing cross-sectional area, A_D, for water-soluble compounds. Hence, we can conclude that the effective affinity of allocrite for ABCB1 as well as for ABCG2 increases (i.e., ΔG^0_{tl1} decreases) with the number of weighted hydrogen bond acceptors per allocrite as demonstrated in panels A and B of Figure 2. For both transporters, the decrease in the free energy of binding, ΔG^0_{tl1}, is more pronounced at a low number of HBAs and levels off at higher numbers. In addition to hydrogen bond formation, charge effects may play a certain role. For the strongly cationic compounds (**1**, **6**, and **15**) and for the strongly anionic compounds (**20** and **22**), the free energies of binding, ΔG^0_{tl1}, to

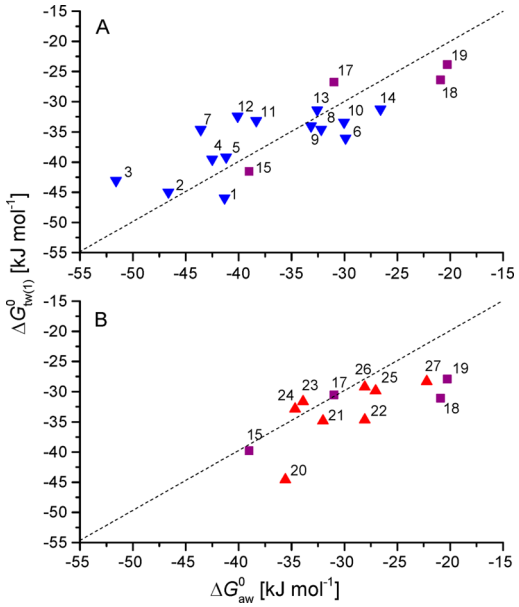

Figure 1. Correlation between the free energy of air−water partitioning of the allocrite, ΔG^0_{aw}, and the free energy of allocrite binding to the first binding site of the transporter, ΔG^0_{tw1}. The dashed lines are diagonals to guide the eye. (A) Compounds activating only ABCB1 (down-triangles, blue) and activating ABCB1 and ABCG2 (squares, violet). (B) Compounds activating only ABCG2 (up-triangles, red) and activating ABCB1 and ABCG2 (squares, violet). Verapamil (**1**), tamoxifen (**2**), Ko143 (**3**), digoxin (**4**), progesterone (**5**), moxifloxacin (**6**), glibenclamide (**7**), promazine (**8**), etoposide (**9**), cortisol (**10**), forskolin (**11**), testosterone (**12**), dexamethasone (**13**), ranitidine (**14**), daunorubicin (**15**), famotidine (**17**), cimetidine (**18**), nizatidine (**19**), sulfasalazine (**20**), mitoxantrone (**21**), CPT-cAMP (**22**), riboflavin (**23**), pefloxacin (**24**), enrofloxacin (**25**), ciprofloxacin (**26**), and norfloxacin (**27**) (for details see Table S1 and Table S1 of ref 20).

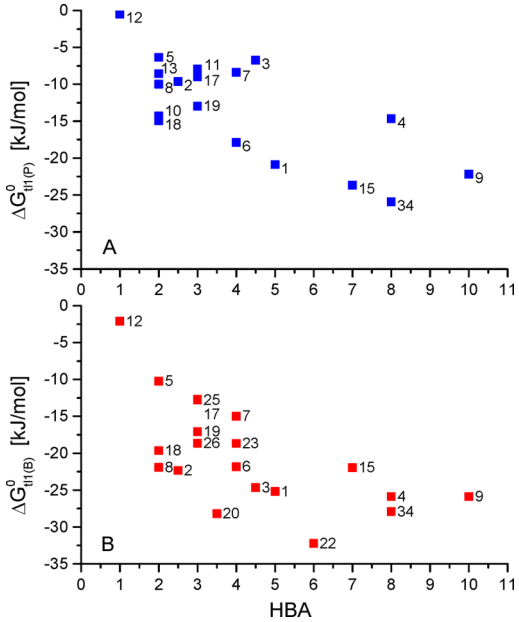

Figure 2. Free energy of allocrite binding from the lipid membrane to ABCB1, $\Delta G^0_{tl(P)}$ (A), and ABCG2, $\Delta G^0_{tl(B)}$, vs weighted HBAs. Compounds (**1**−**26**) are numbered as in legend to Figure 1, C12EO8 (**34**). For details see Table S1 and Table 1, respectively.

DOI: 10.1021/acs.biochem.5b00649
Biochemistry 2015, 54, 6195−6206

ABCB1 and ABCG2, respectively, are more negative than for the remaining compounds that are less charged.

Common Recognition Patterns for ABCB1 and ABCG2. Free electron pairs of nitrogen, oxygen, or sulfur atoms, as well as π-electron systems,[54] can act as HBAs in allocrites. Binding to ABCB1 requires at least two free electron pairs (or HBAs) per allocrite that are arranged at a distance of either ~2.5 Å (type I unit) or ~4.6 Å (type II unit).[26] For the sake of simplicity, we counted the atoms and π-electron systems, carrying HBAs in type I and type II units, not the individual free electron pairs, and arbitrarily weighted them. The weighted HBAs are given in arbitrary energy units (EU). Oxygen was given a weight of EU = 1, and nitrogen, sulfur, and π-electron systems were given a weight of EU = 0.5 (for details, see refs 24 and 26). However, it has to be noted that not all free electron pairs in oxygens, nitrogens, or sulfur atoms are strong enough to interact with ABCB1. Examples of interacting free electron pairs are found in oxygens of carbonyl or ether groups, whereas free electron pairs in oxygens of hydroxyl groups are in most cases too weak to interact with ABCB1. Exceptions may be hydroxyl groups in planar type I or type II patterns (e.g., in daunorubicin). Further examples of interacting free electron pairs are found in nitrogens of tertiary amino groups (but not in secondary and primary amino groups), in sulfur of sulfides or sulfoxides, and in π-electron systems such as phenyl rings.[26]

Transporter ABCC1 (MRP1) has been shown to react with the same molecular recognition patterns (type I and type II units) as ABCB1.[28] The same recognition patterns were recently also demonstrated for ABCG2,[55] which is in agreement with the analysis of HBAs in the present compounds (see Figure 2A,B and Table S1[20]).

Notably, primary and secondary amino groups bind to neither ABCB1[26] nor ABCG2, as was demonstrated, e.g., by the lack of an interaction of rilpivirine or nelfinavir with ABCB1 and ABCG2.[56] In this context, it should be noted that hydroxyl groups as well as primary and secondary amino groups significantly reduce the rate of diffusion of the compound across the lipid membrane and therefore render compounds more prone to an interaction with an exporter, provided they carry interactive HBAs.[57] This effect should not be mistaken for a direct interaction with the transporters.

ABCG2 Binds Its Allocrites More Efficiently Than ABCB1 Does. The free energy of binding from water to the transporter, ΔG^0_{tw1}, is on average more negative for ABCG2 than for ABCB1 as seen in Figure 1A,B. The difference in the free energy of binding of allocrite to ABCB1 (P) and ABCG2 (B), $\Delta\Delta G^0_{tl1,B-P}$, is of particular interest because it may provide more insight into the binding mechanism. The difference in the free energy of allocrite binding from water to the two transporters was obtained by subtracting eq 4 from eq 6

$$\Delta G^0_{tw1,B} - \Delta G^0_{tw1,P} = \Delta\Delta G^0_{tw1,B-P} = \Delta\Delta G^0_{tl1,B-P} \qquad (10)$$

The free energy difference, $\Delta\Delta G^0_{tw1,B-P}$, of allocrite binding from water to the first binding site of ABCB1 and ABCG2 is identical to the free energy difference, $\Delta\Delta G^0_{tl1,B-P}$, of allocrite binding from the lipid membrane to the first binding sites of ABCB1 and ABCG2, because the free energy of allocrite partitioning into the lipid membrane, ΔG^0_{lw}, is identical for plasma membranes of NIH-MDR1-G185 and ABCG2-M-ATPase membranes, to a first approximation.[47] An analogous equation can be written for the second binding site.

Assuming that the primary binding step is due essentially to the formation of hydrogen bonds between HBAs in allocrites and HBDs in the TMDs of the transporters (see below), we plotted the difference in the free energies of allocrite binding between the two transporters, normalized to one HBA, $\Delta\Delta G^0_{HBA,B-P}$, as a function of the number of weighted HBAs per allocrite (Figure 3A). For the majority of allocrites, the free energy difference of

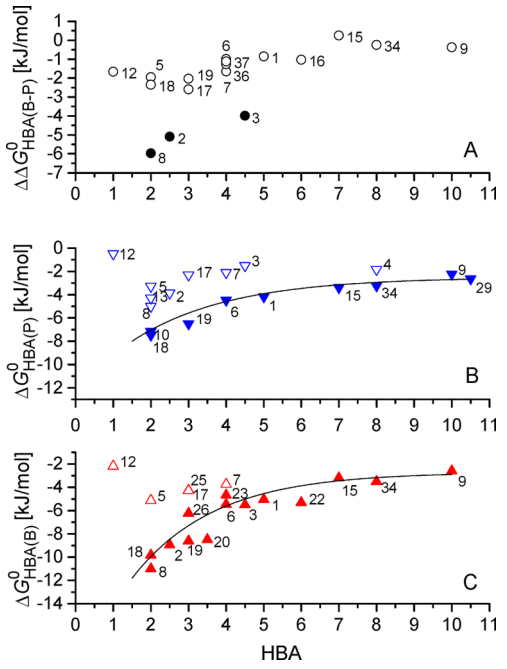

Figure 3. Free energy of binding per HBA in allocrites to ABCB1, $\Delta G^0_{HBA,P}$, and ABCG2, $\Delta G^0_{HBA,B}$, as a function of the number of weighted HBAs per allocrite. (A) Difference in the free energy of binding to ABCG2 and ABCB1, $\Delta\Delta G^0_{HBA(B-P)}$ (filled and open circles, black). Filled symbols are compounds with particularly high differences in free energies of binding, $\Delta\Delta G^0_{HBA(B-P)}$. (B) Free energy of binding per HBA in allocrite to ABCB1, $\Delta G^0_{HBA,P}$ (filled and open down-triangles, blue). (C) Free energy of binding per HBA in allocrite to ABCG2 $\Delta G^0_{HBA,B}$ (filled and open up-triangles, red). Filled symbols in (B) and (C) are compounds with comparatively high affinity to transporters. Numbering from **1**–**39** corresponds to numbering in Figure 1, Table S1, and Table 1.

allocrite binding per hydrogen bond to ABCB1 and ABCG2 ranged from $\Delta\Delta G^0_{HBA,P-B} = -1.9$ to -0.3 kJ/mol and became less negative with an increasing number of HBAs. Exceptionally large differences, $\Delta\Delta G^0_{HBA,B-P}$, were observed for the inhibitor Ko 143 ($\Delta\Delta G^0_{HBA,B-P} \sim -3$ kJ/mol), promazine ($\Delta\Delta G^0_{HBA,B-P} \sim -6$ kJ/mol), and tamoxifen ($\Delta\Delta G^0_{HBA,B-P} \sim -7$ kJ/mol). Notably, the large difference in free energies of allocrite binding to the two transporters is not due to a particularly high affinity of promazine, tamoxifen, and Ko 143 for ABCG2 (see Figure 3C), but rather to their comparatively low affinity for ABCB1 (see Figure 3B).

The Free Energy of Binding per Hydrogen Bond Acceptor Varies Differently for the Two Transporters. The free energy of allocrite binding from the lipid phase to the transporter, ΔG^0_{tl}, cannot be measured directly. However, the value is accessible as the difference between the free energy of transporter–water binding, $\Delta G^0_{tw1,B}$, and the free energy of lipid–water partitioning, ΔG^0_{lw} (see eqs 4 and 6). The former was derived from the concentration of half-maximal activation, K_I (see eq 3). The latter was determined according to eq 5, using the

DOI: 10.1021/acs.biochem.5b00649
Biochemistry 2015, 54, 6195–6206

air−water partition coefficient, K_{aw}, and the cross-sectional area, A_D, as parameters taken from Table S1.

For compounds that show no pronounced ABCG2−ATPase activation (see Table 1, compounds **1**−**14** in ref 20), the concentration of half-maximal activation, K_1, and as a consequence the free energy of binding to the transporter, ΔG^0_{tl1}, cannot be assessed according to eqs 4 and 6. As an alternative, we estimated the free energy of binding to ABCG2, $\Delta G^0_{tl,B}$, as the sum of the free energy of binding to ABCB1, $\Delta G^0_{tl,P}$, and the difference in the free energy of binding between the two transporters, $\Delta\Delta G^0_{tl2,B-P}$

$$\Delta G^0_{tl1,B} \approx \Delta G^0_{tl1,P} + \Delta\Delta G^0_{tl2,B-P} \quad (11)$$

This is possible because the free energy differences for the first, $\Delta\Delta G^0_{tl1,B-P}$, and second binding sites, $\Delta\Delta G^0_{tl2,B-P}$, of the two transporters are comparable.

Panels B and C of Figure 3 show the free energy of binding of allocrite to the transporter, normalized to one weighted HBA in an allocrite, ΔG^0_{HBA}, as a function of the number of weighted HBAs. For ABCB1 (Figure 2B), the free energy per weighted HBA ranged typically from $\Delta G^0_{HBA} \approx -8$ to -2.5 kJ/mol, becoming less negative (i.e., less effective) with an increasing number of HBAs per allocrite. These values are in close agreement with data from a previous investigation performed under identical experimental conditions.[40] Notably, the very hydrophobic compounds with a low number of HBAs [testosterone (**12**) and progesterone (**5**) in Figure 3B] tend to remain in the lipid phase. For these compounds, the free energy of binding to the membrane is more negative than the free energy of binding to ABCB1 (see Figure 5 of ref 24). Hence, hydrophobic elements in allocrites lead to allocrite accumulation in the membrane but do not contribute to direct allocrite−ABCB1 interactions (see eqs 4 and 6).

An analogous plot for ABCG2 (Figure 3C) shows that the free energies of binding per HBA range from $\Delta G^0_{HBA,B} \approx -12$ to -2.5 kJ/mol. Values were thus distinctly more negative for ABCG2 than for ABCB1, at least at low numbers of HBAs per allocrite (HBA ≤ 5); at larger numbers, the difference leveled off. As most compounds on the fitting line in Figure 3C, promazine, tamoxifen, and Ko 143, comprise at least two unsaturated rings in a planar arrangement. This suggests the possibility of additional favorable $\pi-\pi$ stacking interactions (i.e., weak electrostatic interactions) between allocrites and ABCG2 that are however most likely weaker than hydrogen bonding interactions.

Ample Opportunities for Hydrogen Bond Formation in TMDs. HBDs in TMDs most likely play a dual role; on one hand, they extract compounds with appropriate HBAs (allocrites) out of the lipid membrane, and on the other, they guide allocrite sliding across the membrane. To find the potential binding partners for HBAs in allocrites, we screened the TMDs of both transporters for amino acids residues with HBD side groups. Figure 4A−D highlights the amino acid residues carrying HBDs in two conformations of ABCB1, the inward-facing conformation from the crystal structure of apo-Abcb1a (PDB entry 4m1m) and the outward-facing conformation in a homology model based on the crystal structure of Sav1866 (PDB entry 2hyd). The side views (Figure 4A,B) and top views (Figure 4C,D) show a high density of HBDs flanking the pathway across the membrane. Details of the amino acid residues selected are given in Table S2.

In the structure and model used, the HBDs found at the level of the cytosolic lipid headgroups are essentially oriented toward

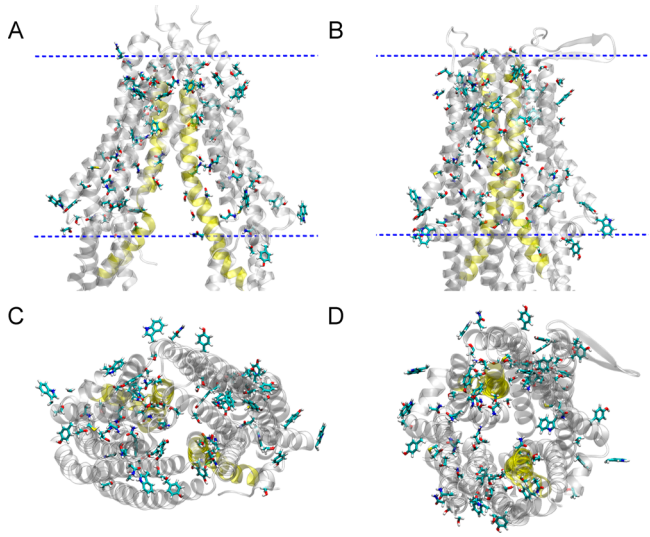

Figure 4. Amino acid residues with HBD side chains of ABCB1 at the level of the membrane (NBDs are truncated). (A) Abcb1a structure of the apo conformation open to the cytosol[14] (PDB entry 4m1m) (side view). (B) Model of the closed conformation, based the crystal structure of Sav1866 with two nucleotides bound[43] (PDB entry 2hyd) (side view). (C) Apo conformation in a top view. (D) Model of the closed conformation in a top view. Amino acid side chains with HBDs are shown. TMD6 and TMD12 are colored yellow, whereas other helices are colored light gray. The two dashed lines indicate the position of the membrane.

the lipid membrane, as observed previously,[58] suggesting attraction of allocrites from the lipid bilayer to the transporter (Figure S2A,D). Closer to the membrane median (Figure S2B,E), HBDs are rather oriented toward the center of the translocation pathway. At the extracellular side of the membrane, HBDs are again oriented partially toward the lipid membrane, most likely to draw allocrites out of the transporter and release them back to the membrane (Figure S2C,F). The weak electrostatic interactions described are assumed to be transient.

To elucidate the allocrite binding sites on ABCB1, Ambudkar and co-workers[59] substituted residues of the binding region (Tyr307, Gln725, and Val982) with Cys in a cysless ABCB1. In these mutant transporters, certain drugs could no longer bind at their primary binding sites but nevertheless modulate ATP hydrolysis, which implies that they bound at secondary sites. These observations are consistent with the results from the structural analysis presented here, suggesting a high redundancy with respect to different weak electrostatic interactions contributing to allocrite binding and gliding in ABCB1.

For ABCG2, high-resolution structures are not yet available, and because of the low level of sequence identity in TMDs, the construction of a homology model would be precarious. We therefore resorted to the putative transmembrane domains of ABCG2. The amino acid residues selected are given in the Supporting Information (Table S1) in comparison to previous investigations.[10,17] The analysis shows that numerous potential anchor points for transient hydrogen bond formation with the HBAs of allocrites are available and allow for a wide range of possible binding as well as gliding combinations. Despite the negligibly low level of sequence identity in the TMDs, the two proteins thus share the same type of allocrite binding mechanism. A functional rather than sequence conservation of residues was also observed for MsbA, Sav1866, and LmrA transporters.[60]

DOI: 10.1021/acs.biochem.5b00649
Biochemistry 2015, 54, 6195−6206

Water as a Model for Allocrites. An allocrite molecule comprises several HBAs, each of which could interact with a binding partner, suggesting the existence of clusters of HBDs arranged in rather close proximity to each other. By scrutinizing the protein−water hydrogen bond network in the 200 ns simulations of apo-ABCB1, we identified two examples of such clusters (Figure 5A−C): Tyr949-Tyr946-Gln942 and Thr841-Ser725-Ser975. Both HBD clusters could form a hydrogen bond network with three water molecules in a water chain. The water chain resembles an allocrite with respect to its ability to offer HBAs to form hydrogen bonds with the transporter. The analysis supports the idea of binding and gliding of allocrites by forming and breaking hydrogen bond interactions.

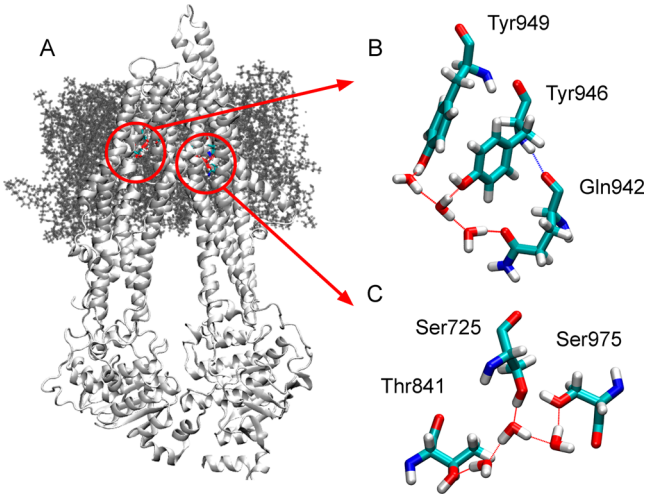

Figure 5. Groups of HBDs that could bind to the same allocrite molecule revealed by the protein−water hydrogen bond network. (A) Snapshot after 200 ns simulations of apo-ABCB1 starting from the crystal structure (PDB entry 3g5u). (B) Hydrogen bond network among Tyr949, Tyr946, Gln942, and three water molecules. (C) Hydrogen bond network among Ser725, Thr841, Ser975, and three water molecules. Gray sticks represent lipids, red dashed lines hydrogen bonds in which hydrogen atoms are offered by oxygens, and blue dashed lines other hydrogen bonds.

Whereas oxygen in water (H−O−H) can offer two HBAs and two HBDs, allocrites generally offer more HBAs than HBDs.[26] Even more importantly, HBAs in allocrites exhibit a higher electron donor strength (R−O−R, R = O or -NR_3) than HBAs in water, because of the positive inductive effect of carbon-containing residues (-R) adjacent to oxygen.

Hydrogen Bond Donors in ABCG2 Are More Potent. To identify the reason for the different allocrite affinities, we analyzed the TMDs of both transporters in more detail. Figure 6 displays the specific amino acid residues with HBD side groups in order of decreasing hydrogen bond donor strength: Cys > Tyr > Trp > Asn > Gln > Ser > Thr (*x*-axis). The order of the HBD strength of the different amino acid residues was obtained by considering the inductive effects of the atoms next to the C atom to which the HBD is attached. Thereby, we did not take into account the fact that Asn and Gln exhibit two HBDs (-NH_2), whereas the other HBDs exhibit only one HBD (-OH, ═NH, or -SH). The abundance of the different amino acid residues in TMDs of the two transporters is given on the *y*-axis (Figure 6).

The total number of amino acid residues with HBD side chains is only slightly higher for ABCG2 (109) than for ABCB1 (104). However, residues with stronger HBD potency, including Cys, Trp, Asn, and Gln, are distinctly more abundant in ABCG2 (10, 19, 17, 15) than in ABCB1 (3, 17, 12, 12). Conversely, residues with lower HBD potency, Ser and Thr, are more abundant in ABCB1 (28, 24) and less abundant in ABCG2 (23, 17). The higher abundance of strong HBDs in ABCG2 may explain the higher affinity per HBA in allocrites. The strong tendency of ABCG2 to extract allocrites with aromatic residues out of the lipid membrane may be due to the high abundance of Tyr.

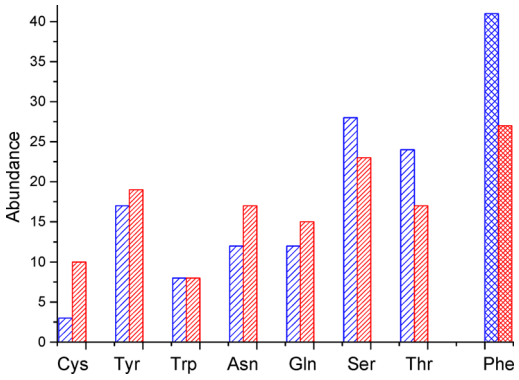

Figure 6. Comparison of ABCB1 (human)[14] and ABCG2 (human)[10,17] with respect to the abundance of the different amino acid residues with HBD side groups. Amino acid residues on the *x*-axis are listed in order of decreasing HBD strength. ABCB1 (blue) and ABCG2 dimer (red).

HBAs and to a certain extent even π-electron systems in allocrites can be considered as "lipophobic" elements, which drive an allocrite from the lipid phase with its low dielectric constant toward HBDs or the π-electron systems in the TMDs of the transporters. Alternatively, HBDs and π-electron systems in the TMDs can be considered as attracting allocrites from the lipid phase, providing the driving force for the "vacuum cleaner".[61] Here we show that because of the higher HBD strength, especially the dominance of Cys and Tyr versus Ser and Thr residues, ABCG2 has a "suction power" that is stronger than that of ABCB1.

ABCB1 Contains More Phenyl Residues. The abundance of Phe was investigated, because π-electron systems are involved in different types of weak electrostatic interactions, such as $\pi-\pi$ and π−cation interactions.[62] The Phe residues in ABCB1 are shown in the inward-facing conformation from the crystal structure of apo-Abcb1a (PDB entry 4m1m) and the outward-facing conformation modeled, based on the crystal structure of Sav1866 (PDB entry 2hyd) (Figure 7A−D). The abundance of Phe was distinctly higher in ABCB1 (**41**) than in ABCG2 (**27**) (see Figure 6). The high efficiency of ABCG2 to extract molecules comprising planar π-electron systems out of the membrane suggests that this is rather due to Tyr. Phe in ABCB1 may rather be involved in binding and transport of cationic allocrites, particularly if they lack HBAs, as, e.g., tetradecyl trimethylammonium chloride (TTAC) and its analogues.[23] The π−cation interactions are weak and may therefore be suited for allocrite transport as shown previously for the transport of ammonium.[63]

Charge−Charge Interactions Play a Role in Transporter Sensing and Gating. The distinctly cationic compounds show an affinity for ABCB1 slightly higher than that of the weakly basic molecules (including those showing a strong pK_a shift upon membrane insertion such as tamoxifen) or electrically neutral molecules (Figure 2A). This is consistent with the observation that the cationic tetradecyl trimethylammonium chloride (TTAC) and its analogues[23] bind to ABCB1, despite

DOI: 10.1021/acs.biochem.5b00649
Biochemistry 2015, 54, 6195−6206

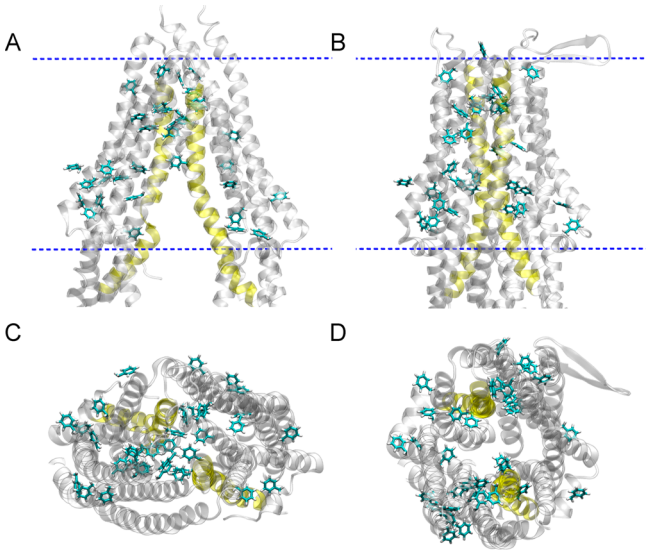

Figure 7. Phenyl residues of ABCB1 at the level of the membrane (NBDs are truncated). The arrangement of figures and representations of membrane position as well as helices are the same as in Figure 4. For the sake of clarity, only side chains of phenyl residues are highlighted.

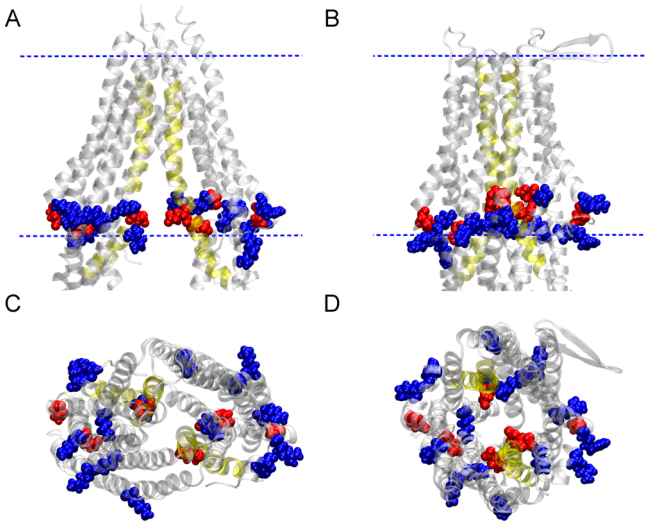

Figure 8. Charged residues of ABCB1 at the cytosolic membrane interface (NBDs are truncated). The arrangement of figures and representations of membrane position as well as helices are the same as in Figure 4. Cationic amino acid residues are colored blue, whereas anionic amino acid residues are colored red.

lacking HBAs. As seen in Figure 2B, the distinctly negatively charged compounds, such as sulfasalazine and CPT-cAMP, show an affinity for ABCG2 slightly higher than that of the weakly charged compounds. These observations suggest that charge plays a certain role in binding to transporters ABCB1 and ABCG2. The somewhat higher affinity of charged residues for the respective transporters in the membrane is, however, compensated by the lower lipid−water partition coefficient of charged compounds. This explains why the influence of charge in binding to ABCB1 was barely noticed.[27,64]

To obtain further insight into the role of charge in allocrite sensing and binding, we investigated the distribution of charged residues in the TMDs of both transporters at the membrane−water interface, assumed to be adjacent to the binding location of allocrites. Figure 8 shows charged residues at the interfacial region of the crystal structure of apo-Abcb1a (Figure 8A,C) and the molecular model of ABCB1, based on the outward-facing structure of Sav1866, bound with ADP (PDB entry 2hyd) in a side view (Figure 8B,D). Fifteen cationic and seven anionic residues were found at the level of the cytosolic membrane−water interface for ABCB1 (see Table S3). The high density of cationic groups at the membrane−water interface of ABCB1 seems surprising at first site but may be relevant for preventing the leak of cationic groups to the cytosol, on one hand, and for guiding ionic groups to the appropriate TM helices, on the other. It is interesting to note that the access routes to TM 6 and TM 12, which are assumed to be most relevant for flopping or transport,[65] are gated by a combination of anionic and cationic residues. They most likely induce charge specificity and limit the access to electrically neutral, cationic, and mildly anionic ($pK_a \geq 6.0$) allocrites. Compounds with lower pK_a values (i.e., stronger negative charge) are excluded, unless they carry sufficient HBAs that can overcompensate for the repulsive forces by hydrogen bond formation.[26] Two molecules that exemplify the subtle balance between electrostatic and hydrogen bonding interactions are listed in Tables 1 and 2 [*n*-octylphosphocholine (fos-choline-8) and 1,2-diheptanoyl-*sn*-glycero-3-phosphocholine (DHPC)].

For ABCG2, we again resorted to the putative transmembrane domains of ABCG2[10,17] and determined the putative interfacial charged amino acid residues. Only one cationic residue (R482 in TM3) was found in the interfacial region of an ABCG2 monomer and thus two in the homodimer, compared to 22 charged residues in ABCB1 (see Table S3). The two cationic residues are consistent with the ability of ABCG2 to transport anionic compounds. The lower putative interfacial charge density in ABCG2 may explain the higher promiscuity toward highly charged (zwitterionic, double cationic, and double anionic) allocrites.[20] In summary, this analysis suggests that charge−charge interactions play a particular role in sensing and gating, and to a lower extent also in allocrite binding. The network of possible attractive and repulsive electrostatic interactions differs in the two proteins and gives rise to allocrite specificity.

CONCLUSIONS

Despite the relative hydrophilicity of ABCG2-activating allocrites, binding occurs in the cytosolic membrane leaflet as for ABCB1. The binding location is consistent with the function of the two transporters to ward off compounds before they enter the cytosol. Hence, allocrite binding for ABCG2 is a two-step process, starting with allocrite partitioning into the lipid membrane driven by hydrophobic interactions, followed by binding of allocrite to the TMDs, driven essentially by weak electrostatic interactions between HBAs in allocrites and HBDs in the transmembrane region of both transporters. The weak electrostatic or "lipophobic" interactions may further include $\pi-\pi$ stacking and π−cation interactions. The former may be particularly relevant for binding of planar π-electron systems by ABCG2, whereas the latter may be particularly relevant for cation transport by ABCB1. The common membrane-mediated allocrite binding mechanism provides transporter promiscuity and allocrite overlap. Notably, ABCG2 binds its allocrites with an affinity higher than that of ABCB1, which is most likely due to the overall higher hydrogen bond donor strength of HBDs in ABCG2. The different affinities add a tuning element to promiscuity and facilitate a certain division of labor in membranes with ABCB1 and ABCG2. ABCB1, working faster,[20] may become activated at high allocrite concentrations and may rapidly remove allocrites to a level at which the slower ABCG2

DOI: 10.1021/acs.biochem.5b00649
Biochemistry 2015, 54, 6195−6206

becomes activated and can remove the reminders. Attractive as well as repulsive electrostatic interactions between charged groups in allocrites and charged residues in the TMDs of the transporters at the level of the cytosolic lipid−water interface play a major role in allocrite sensing and gating. ABCG2 seems to exhibit a charge density at the interface lower than that of ABCB1, which may explain the higher tolerance to allocrites' amphiphilicity and charge. Transporter specificity is thus due essentially to ionized amino acid residues at the level of the cytosolic membrane−water interface.

■ ASSOCIATED CONTENT

Supporting Information

The Supporting Information is available free of charge on the ACS Publications website at DOI: 10.1021/acs.biochem.5b00649.

Physicochemical characterization of the compounds presented here (data taken from ref 20) (Table S1), sequences of the different helices in ABCB1 at the transmembrane level and the corresponding sequence segments of ABCG2 (Table S2), amino acid sequences of the transmembrane helices in ABCB1 at the membrane−cytosol interface and the corresponding sequence segments of ABCG2 (Table S3), free energies of binding of allocrite to the transporter in the lipid membrane versus the cross-sectional area of the molecule at the air−water interface, A_D, and the correlation between weighted HBAs and the cross-sectional area of the molecules, A_D, at the air−water interface (Figure S1), and amino acid residues with HBDs at different levels of the transmembrane part of apo-Abcb1a (PDB entry 4m1m; NBDs are truncated) (PDF)

■ AUTHOR INFORMATION

Corresponding Author

*Telephone: +41-61-267 22 06. Fax: +41-61-267 21 89. E-mail: anna.seelig@unibas.ch.

Author Contributions

Y.X. and E.E. contributed equally to this work.

Funding

This work was supported by Swiss National Science Foundation Grant 31003A-129701 to A.S. and SNF-Professorship 139205 to S.B. Y.X. was supported by the China Scholarship Council. E.E. was supported by a predoctoral grant from Junta de Castilla y León (European Social Fund). Computational resources were provided through a grant from the Swiss National Supercomputing Centre (CSCS) under Project ID s241.

Notes

The authors declare no competing financial interest.

■ ACKNOWLEDGMENTS

We are grateful to Dr. Claudia Hornung and Dr. Hans-Joachim Schönfeld for helpful discussions regarding the hydrogen bond donor strength of amino acid residues.

■ REFERENCES

(1) Doyle, L. A., Yang, W., Abruzzo, L. V., Krogmann, T., Gao, Y., Rishi, A. K., and Ross, D. D. (1998) A multidrug resistance transporter from human MCF-7 breast cancer cells. *Proc. Natl. Acad. Sci. U. S. A. 95*, 15665−15670.

(2) Ling, V., and Baker, R. M. (1978) Dominance of colchicine resistance in hybrid CHO cells. *Somatic Cell Genet. 4*, 193−200.

(3) Gottesman, M. M., Fojo, T., and Bates, S. E. (2002) Multidrug resistance in cancer: role of ATP-dependent transporters. *Nat. Rev. Cancer 2*, 48−58.

(4) Ni, Z., Bikadi, Z., Rosenberg, M. F., and Mao, Q. (2010) Structure and function of the human breast cancer resistance protein (BCRP/ABCG2). *Curr. Drug Metab. 11*, 603−617.

(5) Mao, Q., and Unadkat, J. D. (2005) Role of the breast cancer resistance protein (ABCG2) in drug transport. *AAPS J. 7*, E118−E133.

(6) Sarkadi, B., Homolya, L., Szakacs, G., and Varadi, A. (2006) Human multidrug resistance ABCB and ABCG transporters: participation in a chemoimmunity defense system. *Physiol. Rev. 86*, 1179−1236.

(7) Robey, R. W., To, K. K., Polgar, O., Dohse, M., Fetsch, P., Dean, M., and Bates, S. E. (2009) ABCG2: a perspective. *Adv. Drug Delivery Rev. 61*, 3−13.

(8) Holland, I. B., and Blight, M. A. (1999) ABC-ATPases, adaptable energy generators fuelling transmembrane movement of a variety of molecules in organisms from bacteria to humans. *J. Mol. Biol. 293*, 381−399.

(9) Szakacs, G., Paterson, J. K., Ludwig, J. A., Booth-Genthe, C., and Gottesman, M. M. (2006) Targeting multidrug resistance in cancer. *Nat. Rev. Drug Discovery 5*, 219−234.

(10) Jani, M., Ambrus, C., Magnan, R., Jakab, K. T., Beery, E., Zolnerciks, J. K., and Krajcsi, P. (2014) Structure and function of BCRP, a broad specificity transporter of xenobiotics and endobiotics. *Arch. Toxicol. 88*, 1205−1248.

(11) Ni, Z., Mark, M. E., Cai, X., and Mao, Q. (2010) Fluorescence resonance energy transfer (FRET) analysis demonstrates dimer/oligomer formation of the human breast cancer resistance protein (BCRP/ABCG2) in intact cells. *Int. J. Biochem Mol. Biol. 1*, 1−11.

(12) Xu, J., Peng, H., Chen, Q., Liu, Y., Dong, Z., and Zhang, J. T. (2007) Oligomerization domain of the multidrug resistance-associated transporter ABCG2 and its dominant inhibitory activity. *Cancer Res. 67*, 4373−4381.

(13) McDevitt, C. A., Collins, R. F., Conway, M., Modok, S., Storm, J., Kerr, I. D., Ford, R. C., and Callaghan, R. (2006) Purification and 3D structural analysis of oligomeric human multidrug transporter ABCG2. *Structure 14*, 1623−1632.

(14) Aller, S. G., Yu, J., Ward, A., Weng, Y., Chittaboina, S., Zhuo, R., Harrell, P. M., Trinh, Y. T., Zhang, Q., Urbatsch, I. L., and Chang, G. (2009) Structure of P-glycoprotein reveals a molecular basis for poly-specific drug binding. *Science 323*, 1718−1722.

(15) Li, J., Jaimes, K. F., and Aller, S. G. (2014) Refined structures of mouse P-glycoprotein. *Protein science: a publication of the Protein Society 23*, 34−46.

(16) Kodan, A., Yamaguchi, T., Nakatsu, T., Sakiyama, K., Hipolito, C. J., Fujioka, A., Hirokane, R., Ikeguchi, K., Watanabe, B., Hiratake, J., Kimura, Y., Suga, H., Ueda, K., and Kato, H. (2014) Structural basis for gating mechanisms of a eukaryotic P-glycoprotein homolog. *Proc. Natl. Acad. Sci. U. S. A. 111*, 4049−4054.

(17) Rosenberg, M. F., Bikadi, Z., Chan, J., Liu, X., Ni, Z., Cai, X., Ford, R. C., and Mao, Q. (2010) The human breast cancer resistance protein (BCRP/ABCG2) shows conformational changes with mitoxantrone. *Structure 18*, 482−493.

(18) Kodaira, H., Kusuhara, H., Ushiki, J., Fuse, E., and Sugiyama, Y. (2010) Kinetic analysis of the cooperation of P-glycoprotein (P-gp/Abcb1) and breast cancer resistance protein (Bcrp/Abcg2) in limiting the brain and testis penetration of erlotinib, flavopiridol, and mitoxantrone. *J. Pharmacol. Exp. Ther. 333*, 788−796.

(19) Polli, J. W., Olson, K. L., Chism, J. P., John-Williams, L. S., Yeager, R. L., Woodard, S. M., Otto, V., Castellino, S., and Demby, V. E. (2009) An unexpected synergist role of P-glycoprotein and breast cancer resistance protein on the central nervous system penetration of the tyrosine kinase inhibitor lapatinib (N-{3-chloro-4-[(3-fluorobenzyl)-oxy]phenyl}-6-[5-({[2-(methylsulfonyl)ethyl]amino }methyl)-2-furyl]-4-quinazolinamine; GW572016). *Drug metabolism and disposition: the biological fate of chemicals 37*, 439−442.

(20) Egido, E., Müller, R., Li-Blatter, X., Merino, G., and Seelig, A. (2015) Predicting Allocrites for the Breast Cancer Resistance Protein (ABCG2) and P-Glycoprotein (ABCB1) Based on Mechanistic

DOI: 10.1021/acs.biochem.5b00649
Biochemistry 2015, 54, 6195−6206

Considerations. *Mol. Pharmaceutics*, DOI: 10.1021/acs.molpharmaceut.5b00463.
(21) Homolya, L., Hollo, Z., Germann, U. A., Pastan, I., Gottesman, M. M., and Sarkadi, B. (1993) Fluorescent cellular indicators are extruded by the multidrug resistance protein. *J. Biol. Chem. 268*, 21493−21496.
(22) Gottesman, M. M., and Pastan, I. (1993) Biochemistry of multidrug resistance mediated by the multidrug transporter. *Annu. Rev. Biochem. 62*, 385−427.
(23) Li-Blatter, X., Beck, A., and Seelig, A. (2012) P-Glycoprotein-ATPase Modulation: The Molecular Mechanisms. *Biophys. J. 102*, 1383−1393.
(24) Gatlik-Landwojtowicz, E., Aanismaa, P., and Seelig, A. (2006) Quantification and characterization of P-glycoprotein-substrate interactions. *Biochemistry 45*, 3020−3032.
(25) Heerklotz, H., and Keller, S. (2013) How membrane partitioning modulates receptor activation: parallel versus serial effects of hydrophobic ligands. *Biophys. J. 105*, 2607−2610.
(26) Seelig, A. (1998) A general pattern for substrate recognition by P-glycoprotein. *Eur. J. Biochem. 251*, 252−261.
(27) Schmid, D., Ecker, G., Kopp, S., Hitzler, M., and Chiba, P. (1999) Structure-activity relationship studies of propafenone analogs based on P-glycoprotein ATPase activity measurements. *Biochem. Pharmacol. 58*, 1447−1456.
(28) Seelig, A., Blatter, X. L., and Wohnsland, F. (2000) Substrate recognition by P-glycoprotein and the multidrug resistance-associated protein MRP1: a comparison. *Int. J. Clin. Pharmacol. Ther. 38*, 111−121.
(29) Omote, H., and Al-Shawi, M. K. (2006) Interaction of Transported Drugs with the Lipid Bilayer and P-Glycoprotein through a Solvation Exchange Mechanism. *Biophys. J. 90*, 4046−4059.
(30) Li-Blatter, X., Nervi, P., and Seelig, A. (2009) Detergents as intrinsic P-glycoprotein substrates and inhibitors. *Biochim. Biophys. Acta, Biomembr. 1788*, 2335−2344.
(31) Li-Blatter, X., and Seelig, A. (2010) Exploring the P-glycoprotein binding cavity with polyoxyethylene alkyl ethers. *Biophys. J. 99*, 3589−3598.
(32) Habazettl, J., Allan, M., Jensen, P. R., Sass, H. J., Thompson, C. J., and Grzesiek, S. (2014) Structural basis and dynamics of multidrug recognition in a minimal bacterial multidrug resistance system. *Proc. Natl. Acad. Sci. U. S. A. 111*, E5498−5507.
(33) Litman, T., Zeuthen, T., Skovsgaard, T., and Stein, W. D. (1997) Structure-activity relationships of P-glycoprotein interacting drugs: kinetic characterization of their effects on ATPase activity. *Biochim. Biophys. Acta, Mol. Basis Dis. 1361*, 159−168.
(34) Loo, T. W., and Clarke, D. M. (1996) Mutational analysis of the predicted first transmembrane segment of each homologous half of human P-glycoprotein suggests that they are symmetrically arranged in the membrane. *J. Biol. Chem. 271*, 15414−15419.
(35) Dey, S., Ramachandra, M., Pastan, I., Gottesman, M. M., and Ambudkar, S. V. (1997) Evidence for two nonidentical drug-interaction sites in the human P-glycoprotein. *Proc. Natl. Acad. Sci. U. S. A. 94*, 10594−10599.
(36) Shapiro, A. B., and Ling, V. (1997) Extraction of Hoechst 33342 from the cytoplasmic leaflet of the plasma membrane by P-glycoprotein. *Eur. J. Biochem. 250*, 122−129.
(37) Shapiro, A. B., and Ling, V. (1997) Positively cooperative sites for drug transport by P-glycoprotein with distinct drug specificities. *Eur. J. Biochem. 250*, 130−137.
(38) Qu, Q., and Sharom, F. J. (2002) Proximity of bound Hoechst 33342 to the ATPase catalytic sites places the drug binding site of P-glycoprotein within the cytoplasmic membrane leaflet. *Biochemistry 41*, 4744−4752.
(39) Lugo, M. R., and Sharom, F. J. (2005) Interaction of LDS-751 with P-glycoprotein and mapping of the location of the R drug binding site. *Biochemistry 44*, 643−655.
(40) Aanismaa, P., and Seelig, A. (2007) P-Glycoprotein Kinetics Measured in Plasma Membrane Vesicles and Living Cells. *Biochemistry 46*, 3394−3404.
(41) Garrigues, A., Nugier, J., Orlowski, S., and Ezan, E. (2002) A high-throughput screening microplate test for the interaction of drugs with P-glycoprotein. *Anal. Biochem. 305*, 106−114.
(42) Matsson, P., Englund, G., Ahlin, G., Bergstrom, C. A., Norinder, U., and Artursson, P. (2007) A global drug inhibition pattern for the human ATP-binding cassette transporter breast cancer resistance protein (ABCG2). *J. Pharmacol. Exp. Ther. 323*, 19−30.
(43) Dawson, R. J., and Locher, K. P. (2006) Structure of a bacterial multidrug ABC transporter. *Nature 443*, 180−185.
(44) Gatlik-Landwojtowicz, E., Aanismaa, P., and Seelig, A. (2004) The rate of P-glycoprotein activation depends on the metabolic state of the cell. *Biochemistry 43*, 14840−14851.
(45) Landwojtowicz, E., Nervi, P., and Seelig, A. (2002) Real-time monitoring of P-glycoprotein activation in living cells. *Biochemistry 41*, 8050−8057.
(46) Ambudkar, S. V., Cardarelli, C. O., Pashinsky, I., and Stein, W. D. (1997) Relation between the turnover number for vinblastine transport and for vinblastine-stimulated ATP hydrolysis by human P-glycoprotein. *J. Biol. Chem. 272*, 21160−21166.
(47) Egido de Frutos, E. (2014) Ph.D. Thesis, Estudio de la function del transportador de membrana ABCG2 mediante comparacion con la glicoproteina-P: Interaccion con antitumorals, antibioticos, hormonas y otros compuestos. Universidad de León: León, Spain.
(48) Fischer, H., Gottschlich, R., and Seelig, A. (1998) Blood-brain barrier permeation: molecular parameters governing passive diffusion. *J. Membr. Biol. 165*, 201−211.
(49) Gerebtzoff, G., Li-Blatter, X., Fischer, H., Frentzel, A., and Seelig, A. (2004) Halogenation of drugs enhances membrane binding and permeation. *ChemBioChem 5*, 676−684.
(50) Meier, M., Blatter, X. L., Seelig, A., and Seelig, J. (2006) Interaction of verapamil with lipid membranes and P-glycoprotein: connecting thermodynamics and membrane structure with functional activity. *Biophys. J. 91*, 2943−2955.
(51) Polli, J. W., Wring, S. A., Humphreys, J. E., Huang, L., Morgan, J. B., Webster, L. O., and Serabjit-Singh, C. S. (2001) Rational use of in vitro P-glycoprotein assays in drug discovery. *J. Pharmacol Exp Ther 299*, 620−628.
(52) Seelig, A. (2007) The role of size and charge for blood-brain barrier permeation of drugs and fatty acids. *J. Mol. Neurosci. 33*, 32−41.
(53) Seelig, A., and Gatlik-Landwojtowicz, E. (2005) Inhibitors of multidrug efflux transporters: their membrane and protein interactions. *Mini-Rev. Med. Chem. 5*, 135−151.
(54) Levitt, M., and Perutz, M. F. (1988) Aromatic rings act as hydrogen bond acceptors. *J. Mol. Biol. 201*, 751−754.
(55) Eric, S., Kalinic, M., Ilic, K., and Zloh, M. (2014) Computational classification models for predicting the interaction of drugs with P-glycoprotein and breast cancer resistance protein. *SAR and QSAR in environmental research 25*, 939−966.
(56) Marzolini, C., Mueller, R., Li-Blatter, X., Battegay, M., and Seelig, A. (2013) The brain entry of HIV-1 protease inhibitors is facilitated when used in combination. *Mol. Pharmaceutics 10*, 2340−2349.
(57) Nervi, P., Li-Blatter, X., Aanismaa, P., and Seelig, A. (2010) P-glycoprotein substrate transport assessed by comparing cellular and vesicular ATPase activity. *Biochim. Biophys. Acta, Biomembr. 1798*, 515−525.
(58) Mandal, D., Moitra, K., Ghosh, D., Xia, D., and Dey, S. (2012) Evidence for modulatory sites at the lipid-protein interface of the human multidrug transporter P-glycoprotein. *Biochemistry 51*, 2852−2866.
(59) Chufan, E. E., Kapoor, K., Sim, H. M., Singh, S., Talele, T. T., Durell, S. R., and Ambudkar, S. V. (2013) Multiple transport-active binding sites are available for a single substrate on human P-glycoprotein (ABCB1). *PLoS One 8*, e82463.
(60) Gutmann, D. A., Ward, A., Urbatsch, I. L., Chang, G., and van Veen, H. W. (2010) Understanding polyspecificity of multidrug ABC transporters: closing in on the gaps in ABCB1. *Trends Biochem. Sci. 35*, 36−42.
(61) Raviv, Y., Pollard, H. B., Bruggemann, E. P., Pastan, I., and Gottesman, M. M. (1990) Photosensitized labeling of a functional

DOI: 10.1021/acs.biochem.5b00649
Biochemistry 2015, 54, 6195−6206

multidrug transporter in living drug-resistant tumor cells. *J. Biol. Chem. 265*, 3975−3980.
(62) Pawagi, A. B., Wang, J., Silverman, M., Reithmeier, R. A., and Deber, C. M. (1994) Transmembrane aromatic amino acid distribution in P-glycoprotein. A functional role in broad substrate specificity. *J. Mol. Biol. 235*, 554−564.
(63) Baday, S., Wang, S., Lamoureux, G., and Berneche, S. (2013) Different hydration patterns in the pores of AmtB and RhCG could determine their transport mechanisms. *Biochemistry 52*, 7091−7098.
(64) Garnier-Suillerot, A., Marbeuf-Gueye, C., Salerno, M., Loetchutinat, C., Fokt, I., Krawczyk, M., Kowalczyk, T., and Priebe, W. (2001) Analysis of drug transport kinetics in multidrug-resistant cells: implications for drug action. *Curr. Med. Chem. 8*, 51−64.
(65) Loo, T. W., and Clarke, D. M. (2001) Cross-linking of human multidrug resistance P-glycoprotein by the substrate, tris-(2-maleimidoethyl)amine, is altered by ATP hydrolysis. Evidence for rotation of a transmembrane helix. *J. Biol. Chem. 276*, 31800−31805.

DOI: 10.1021/acs.biochem.5b00649
Biochemistry 2015, 54, 6195−6206